INORGANIC CHEMISTRY FRONTIERS

RESEARCH ARTICLE

View Article Online
View Journal | View Issue

Check for updates

Cite this: *Inorg. Chem. Front.*, 2025, **12**, 5741

A tri-alkali/alkaline-earth metal fluorophosphate deep-ultraviolet birefringent crystal with coexisting PO_3F and PO_2F_2†

Tao Ouyang,[a,c,d] Ji Qi,[a,c,d] Yanqiang Li,*[a] Shanshan Chen,[a,d] Weiqi Huang,[a,c,d] Zhiyong Bai,[a] Sangen Zhao *[b] and Junhua Luo *[a,d]

Received 20th March 2025,
Accepted 30th April 2025

DOI: 10.1039/d5qi00752f

rsc.li/frontiers-inorganic

Deep-ultraviolet (deep-UV) birefringent crystals capable of generating or modulating deep-UV polarized lights are essential for modern laser technologies. However, there are few commercial deep-UV birefringent crystals, except MgF_2, which exhibit a tiny birefringence of 0.012@532 nm. Herein, by incorporating multiple alkali/alkaline-earth metal elements, the first tri-alkali/alkaline-earth metal fluorophosphate $KBaSr(PO_2F_2)(PO_3F)_2$ (KBSPF) with the coexistence of $(PO_3F)^{2-}$ and $(PO_2F_2)^-$ has been successfully synthesized using the hydrothermal method. Experimental results indicate that KBSPF not only shows a wide transparency window down to the deep-UV spectral region, but also exhibits a relatively large birefringence of 0.042@550 nm, exceeding those of commercial MgF_2 and most alkali/alkaline-earth metal phosphates or fluorophosphates. Theoretical calculations reveal that $(PO_3F)^{2-}$ and $(PO_2F_2)^-$ anions are responsible for the optical properties of KBSPF. Our work not only provides a promising deep-UV birefringent crystal but also offers new insights to enrich the solid-state chemistry of fluorophosphates.

Published on 09 maggio 2025. Downloaded on 06/05/2026 19:58:39.

Introduction

Deep-ultraviolet (deep-UV) birefringent crystals play a crucial role in advancing optical technologies, such as photoemission spectroscopy, laser micromachining, and high-density storage data, by enabling the manipulation of light at wavelengths below 200 nm.[1–3] From an application perspective, a large birefringence is highly desirable, as it allows for more compact and efficient optical devices. To date, commercially available deep-UV birefringent crystals remain extremely scarce, as most crystals with sufficient birefringence are opaque in the deep-UV spectral region. Although MgF_2, the most widely used deep-UV birefringent crystal, exhibits a wide transparency window, it has a tiny birefringence of 0.012@532 nm.[4] Therefore, it is of urgent demand and has importance in developing novel excellent deep-UV birefringent crystals with enhanced birefringence.

In order to achieve large birefringence, researchers have proposed several effective strategies, including introducing planar π-conjugated units,[5,6] metal cations with stereochemically active lone pairs,[7,8] d^0 metal cations exhibiting second-order Jahn–Teller distortions,[9] and d^{10} transition metals.[10,11] However, metal cations with lone pairs or transition metals always narrow the band gap, reducing their suitability for deep-UV applications. In addition, π–π interactions in planar π-conjugated units, such as $(BO_3)^{3-}$, $(CO_3)^{2-}$, and $(NO_3)^-$, lead to significantly lower band gaps compared to non-π-conjugated units like $(BO_4)^{5-}$, $(PO_4)^{3-}$, and $(SO_4)^{2-}$.[12] As a result, non-π-conjugated units are often preferred as the building blocks for deep-UV optical crystals.[12,13] However, non-π-conjugated units inherently exhibit drawbacks of low anisotropy, which limits their ability to achieve large birefringence, as seen in $KLa(PO_3)_4$ (Δn = 0.0084@1064 nm),[14] $Rb_2Ba_3(P_2O_7)_2$ (Δn = 0.002@1064 nm),[15,16] and $RbNaMgP_2O_7$ (Δn = 0.0034@1064 nm).[16] To overcome low-anisotropy constraints, it has been experimentally demonstrated that fluorine-induced structural distortion in regular tetrahedral frameworks can enhance anisotropic polarizability *via* electron density redistribution. Compared to $(BO_4)^{5-}$, $(PO_4)^{3-}$, and $(SO_4)^{2-}$ units, the resultant tetrahedral groups like (BO_xF_{4-x}) (x = 1, 2, 3), (PO_xF_{4-x}) (x = 1, 2, 3), and $(SO_3F)^-$ exhibit greater anisotropic polarizability.[17–19] The

[a]*State Key Laboratory of Functional Crystals and Devices, Fujian Institute of Research on the Structure of Matter, Chinese Academy of Sciences, Fuzhou, Fujian 350002, China*
[b]*Quantum Science Center of Guangdong-Hong Kong-Macao Greater Bay Area (Guangdong), Shenzhen 518045, China*
[c]*College of Chemistry, Fuzhou University, Fuzhou, Fujian 350108, China*
[d]*Fujian College, University of Chinese Academy of Sciences, Fuzhou, Fujian 350002, China*

†Electronic supplementary information (ESI) available. CCDC 2428547. For ESI and crystallographic data in CIF or other electronic format see DOI: https://doi.org/10.1039/d5qi00752f

Published on 09 maggio 2025. Downloaded on 06/05/2026 19:58:39.

corresponding crystals also exhibit enhanced birefringence, such as $KLa(PO_2F_2)_4$ (Δn = 0.019@1064 nm),[20] Cs_2PO_3F (Δn = 0.017@1064 nm),[21] and $Ba(PO_2F_2)$ (Δn = 0.011@1064 nm).[22]

It is well-known that alkali/alkaline-earth metals are beneficial for deep-UV transparency due to their electronic configuration lacking unfavourable d–d or f–f transition. In this work, the first tri-alkali/alkaline-earth metal fluorophosphate, $KBaSr(PO_2F_2)(PO_3F)_2$ (KBSPF), which coexists with $(PO_3F)^{2-}$ and $(PO_2F_2)^-$, has been successfully synthesized *via* the hydrothermal method. Fluorine substitution is beneficial for bandgap widening. In addition, the coexistence of functional anionic groups enhances microscopic anisotropic polarizability, consequently leading to improved birefringence. KBSPF not only demonstrates a wide transparency window down to the deep-UV spectral region, but also exhibits a significant birefringence of 0.042@550 nm.

Results and discussion

Polycrystalline samples of KBSPF were synthesized using the modified hydrothermal method. Single-crystal X-ray diffraction (XRD) analysis reveals that KBSPF crystallizes in the centrosymmetric space group $P2_1/c$ (No. 14) with a = 7.0638(1) Å, b = 7.4306(1) Å, c = 21.3633(3) Å, β = 93.386(1)°, V = 1119.37(3) Å^3, and Z = 4, and detailed crystallographic information is provided in Tables S1–S5.† Within one asymmetric unit, there are one crystallographically unique K atom, one Ba atom, one Sr atom, three P atoms, four F atoms, and eight O atoms. Among them, the P(1) and P(2) atoms are tetrahedrally bonded to three O atoms and one F atom, forming distorted $(PO_3F)^{2-}$ tetrahedra. The other P(3) atom is surrounded by two O atoms and two F atoms, generating the $(PO_2F_2)^-$ tetrahedra. P–O bonds and P–F bonds range from 1.521(2) to 1.586(2) Å and from 1.504(2) to 1.556(2) Å, respectively. As shown in Fig. 1a,

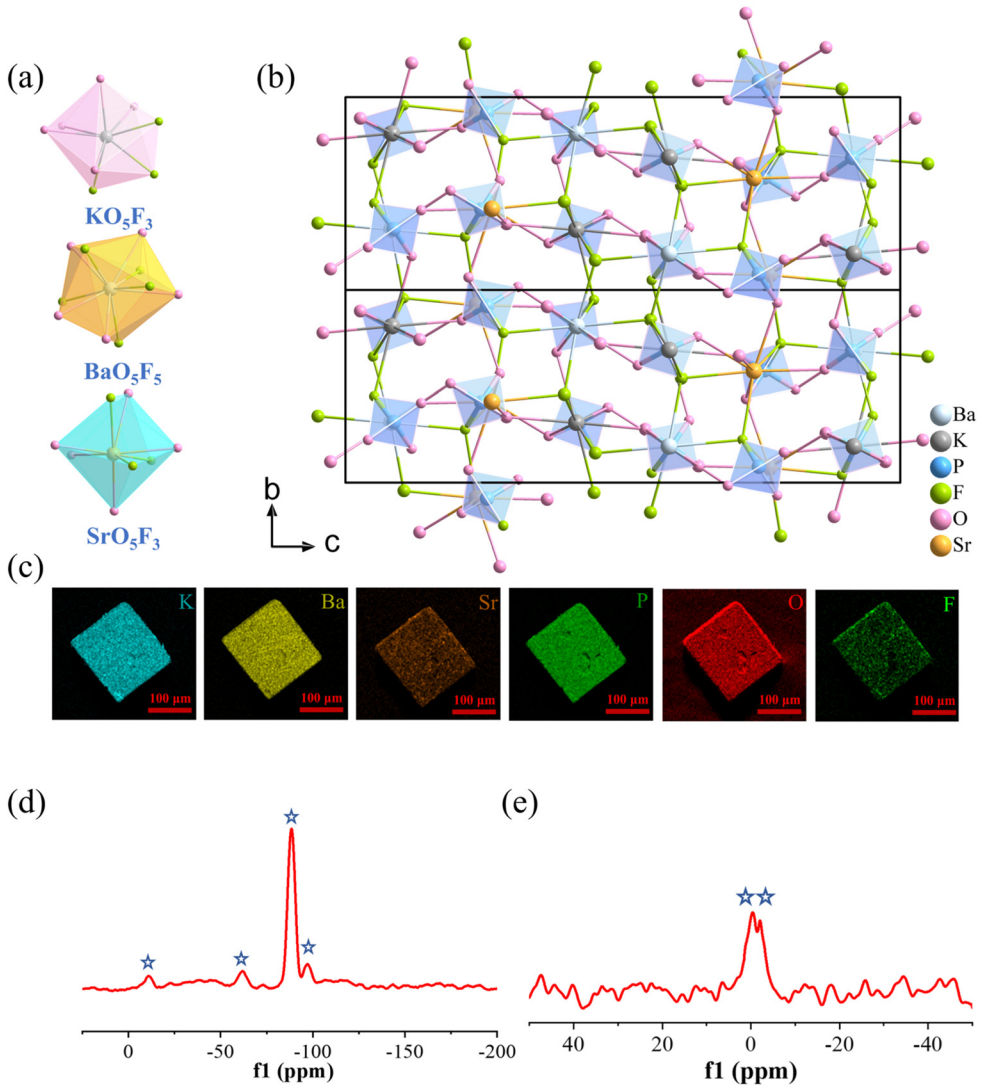

Fig. 1 The crystal structure and elemental characterization of KBSPF. (a) The coordination of K, Ba and Sr. (b) The structure of KBSPF viewed along the *a* axis. (c) Elemental mapping by scanning electron microscopy. (d) ^{19}F NMR spectrum. (e) ^{19}F–^{31}P solid-state cross-polarization NMR spectrum.

 This journal is © the Partner Organisations 2025

Published on 09 maggio 2025. Downloaded on 06/05/2026 19:58:39.

K^+, Sr^{2+}, and Ba^{2+} cations are eight-, eight-, and ten-coordinated, forming KO_5F_3, SrO_5F_3 and BaO_5F_5 cationic polyhedra with bond lengths in the ranges of 2.701(2) to 3.026(2) Å, 2.731(2) to 2.932(2) Å and 2.708(2) to 3.013(2) Å. According to previous reports, all these bond lengths are consistent with previously reported values.[18,22,23] The KO_5F_3, BaO_5F_5 and SrO_5F_3 cationic polyhedra are further interconnected by isolated $(PO_3F)^{2-}$ and $(PO_2F_2)^-$ anionic tetrahedra together *via* corners, edges, and faces, constructing the overall three-dimensional framework with channels (Fig. 1b).

The phase purity of polycrystalline KBSPF was confirmed by the high consistency between the measured and simulated powder XRD patterns, as shown in Fig. S1.† Energy dispersive X-ray spectroscopy (EDS) mapping verified the presence of K, Ba, Sr, P, O, and F elements in a single crystal, with these elements being evenly distributed throughout the crystal (Fig. 1c and S2†). To examine the stability in air, KBSPF was exposed to air for one week. As displayed in Fig. S3† the surface of the exposed crystal is nearly unchanged. Thermogravimetric and differential thermal analyses were performed to evaluate the thermal stability of KBSPF and exclude the possibility of hydroxyl groups (Fig. S4†). KBSPF remains stable up to approximately 573 K, beyond which it undergoes continuous weight loss. To confirm the transmission wave-

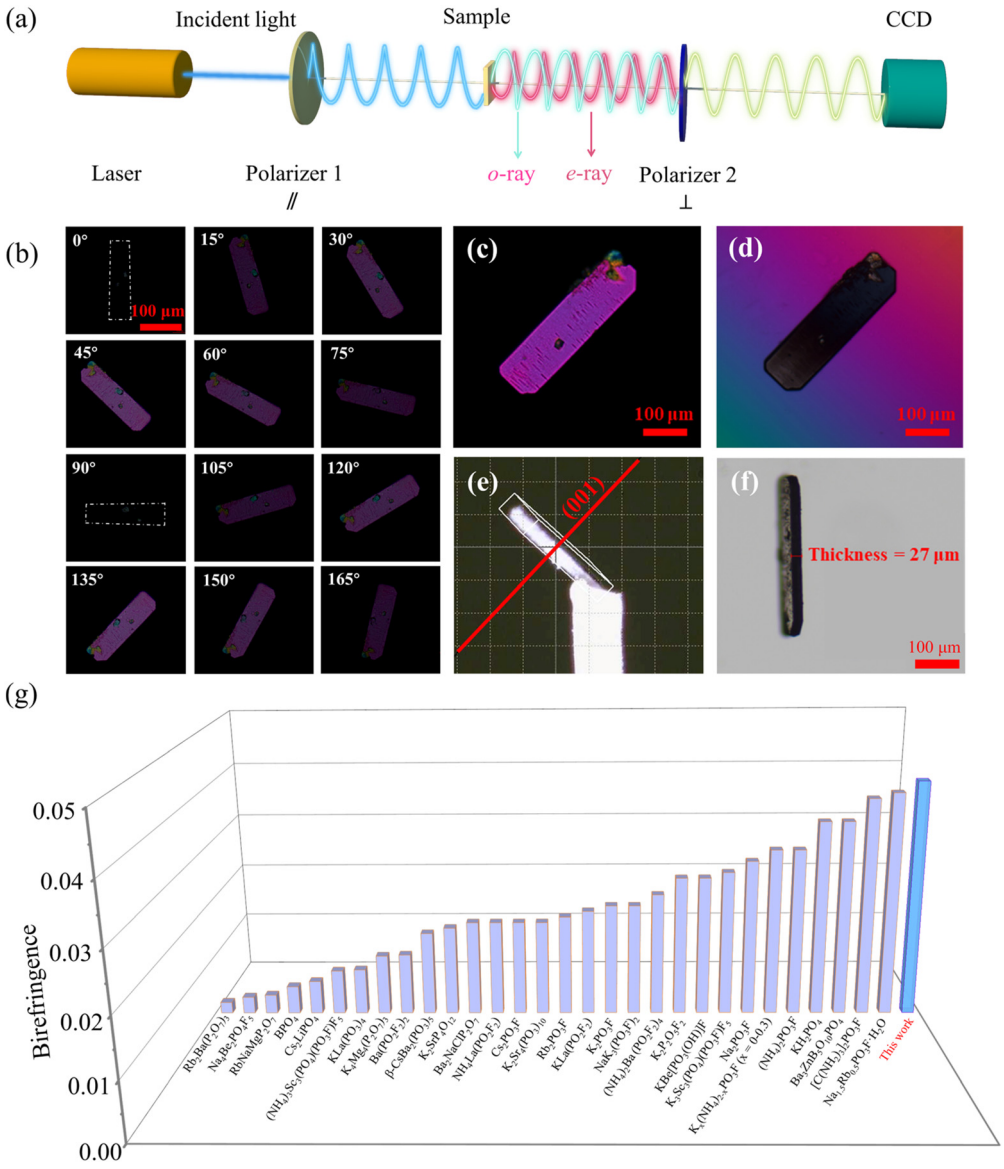

Fig. 2 Birefringence properties of KBSPF. (a) The schematic diagram illustrates the birefringence measurement using a polarizing microscope. (b) Polarized optical observations of a KBSPF crystal. The angle φ at which the KBSPF crystal achieves extinction is defined as 0°. (c) Original interference of the KBSPF crystal under orthogonally polarized light. (d) The corresponding crystal realizing complete extinction. (e) The orientation of the KBSPF plate used for measurement. (f) The thickness of the KBSPF crystal. (g) Comparison of the birefringence of KBSPF with many well-known phosphates and fluorophosphate optical crystals.

Published on 09 maggio 2025. Downloaded on 06/05/2026 19:58:39.

length range of KBSPF, UV/Vis/NIR diffuse reflectance spectra were recorded from 200 to 800 nm. As demonstrated in Fig. S5,† the absorption edge of KBSPF is below 200 nm.

The infrared spectrum of KBSPF is shown in Fig. S6,† and the assignment of related absorption peaks helps identify the corresponding functional units and chemical bonds. The peak at 869 cm^{-1} corresponds to the stretching vibration of the P–F bond. The peak at 496 cm^{-1} corresponds to the vibrational bending of the $(PO_2F_2)^-$ group.[20,22,24] The peak at 430 cm^{-1} corresponds to the vibrational bending of the $(PO_3F)^{2-}$ group.[25,26] To further verify the coexistence of $(PO_3F)^{2-}$ and $(PO_2F_2)^-$ anions, we measured the ^{19}F solid-state nuclear magnetic resonance (NMR) spectrum and ^{19}F–^{31}P solid-state cross-polarization magic angle spinning (MAS) NMR spectrum. The ^{19}F MAS NMR spectrum shows exactly four resonances at δ = −10.91, −61.95, −88.53, and −96.58 ppm (Fig. 1d), which are attributed to the F signals from four different coordination environments.[18] Moreover, the ^{19}F–^{31}P solid-state cross-polarization MAS spectrum reveals two resonances at δ = −0.41 and −2.14 ppm (Fig. 1e), confirming the presence of two distinct P–F bonds in $(PO_3F)^{2-}$ and $(PO_2F_2)^-$ anions.[26]

Given that KBSPF crystallizes in a non-cubic space group, it is expected to be birefringence-active. The experimental birefringence of KBSPF was investigated using a high-quality, colorless crystal plate under an orthogonally polarized microscope. The setup was equipped with a charge-coupled device (CCD) camera to capture transmitted images, as demonstrated in Fig. 2a. Fig. 2b presents transmitted images of the KBSPF crystal under orthogonally polarized light. As the tested single crystal was rotated, the brightness of the transmitted image changed periodically every 45°. This behaviour arises because when the incident polarized light is parallel to the fast or slow axis of the crystal, its polarization state remains perpendicular to the polarizer, resulting in the darkest image. In contrast, when the incident light is oriented at an angle of 45° to the fast or slow axis, the polarized optical images display the greatest brightness of the crystal. These observations confirm that KBSPF has birefringence to modulate the polarization of light.

As shown in Fig. 2c and d, further analysis revealed the original interference colour of second-order purple for the tested single crystal, corresponding to an optical path difference of R = 1095.7 nm, measured using a Berek compensator. The crystal plane of the tested crystal was verified by single-crystal XRD. As depicted in Fig. 2e, the selected crystal plane is along the (001) direction. The thickness of the measured crystal was determined to be d = 27 μm, as shown in Fig. 2f. Therefore, the experimental birefringence was calculated as $\Delta n(001)\text{exp}$ = 0.042@550 nm based on the birefringence formula $\Delta n = R/d$. The calculated wavelength-dependent refractive index at λ = 550 nm is shown in Fig. S7.† The calculated birefringence $\Delta n(001)\text{cal} \approx n[100] - n[010]$ for the (001) crystal plane is 0.042@550 nm (Fig. S7†), which agrees well with the experimental value ($\Delta n(001)\text{exp}$ = 0.042@550 nm). It should be noted that this relatively large birefringence of KBSPF is about four times that of the commercial deep-UV birefringent crystal MgF_2 (Δn = 0.012@532 nm).[27] Moreover, this birefringence far exceeds those of many famous phosphates and fluorophosphate optical crystals (Fig. 2g and Table S6†).[14–16,20–22,23,25,26,28–41]

First-principles calculations were performed to investigate the micro-origin of the optical properties of KBSPF.[42–45] Fig. 3a shows that the electronic band structure of KBSPF is direct,

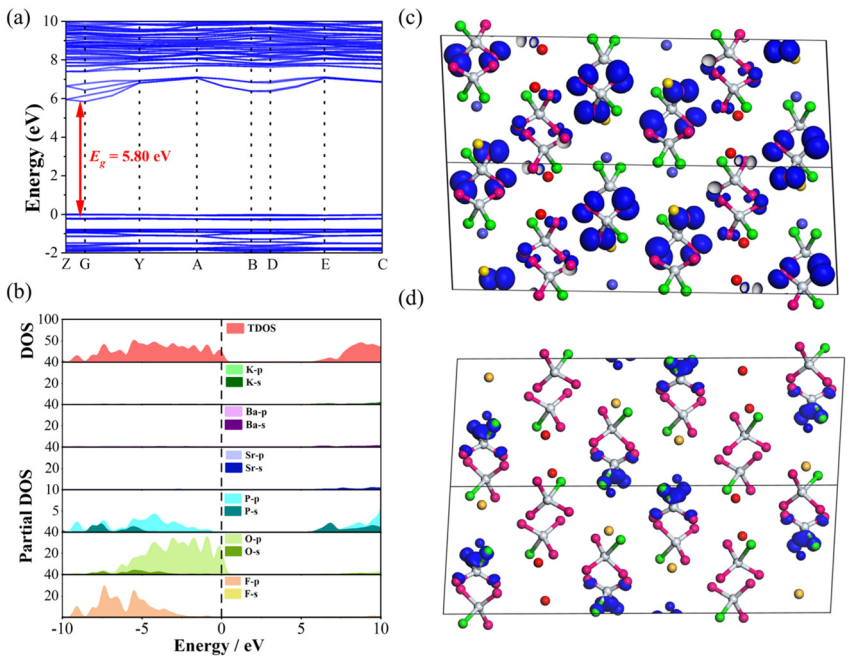

Fig. 3 Theoretical calculations of KBSPF. (a) Electronic band structure. (b) DOS and partial DOS. (c) The HOMO map. (d) The LUMO map. The atoms K, Ba, Sr, P, O and F are denoted using yellow, blue, red, grey, pink, and green balls, respectively.

 This journal is © the Partner Organisations 2025

Published on 09 maggio 2025. Downloaded on 06/05/2026 19:58:39.

with a bandgap of 5.80 eV, in good agreement with the experimental result. The density of states (DOS) and partial DOS for KBSPF (Fig. 3b) indicate that O 2p orbitals predominantly occupy the top part of the valence band. Additionally, P 3p, O 2p, and F 2p orbitals are mainly positioned at the bottom of the conduction band. The highest occupied molecular orbital (HOMO) and lowest unoccupied molecular orbital (LUMO) for KBSPF were also calculated. Fig. 3c and d show that the HOMO is dominated by O 2p orbitals, while the LUMO is mainly composed of P 3p, O 2p and F 2p orbitals. All these calculations indicate that $(PO_3F)^{2-}/(PO_2F_2)^-$ anions contribute dominantly to the optical properties of KBSPF.

Conclusion

In summary, by incorporating multiple alkali and alkaline-earth metal elements, we have successfully synthesized and reported the first tri-alkali/alkaline-earth fluorophosphate, namely $KBaSr(PO_2F_2)(PO_3F)_2$. This compound also represents a rare example of a material, in which both $(PO_3F)^{2-}$ and $(PO_2F_2)^-$ anions coexist. $KBaSr(PO_2F_2)(PO_3F)_2$ demonstrates a wide transparency window down to the deep-UV spectral region and exhibits significant birefringence (0.042@550 nm), surpassing those of most alkali/alkaline-earth metal phosphates and fluorophosphates. The absence of d–d/f–f electron transitions in Ba^{2+} and Sr^{2+} cations enables an enlarged band gap. Furthermore, fluorine substitution not only further widens the band gap but also enhances the anisotropy of microscopic polarizability in the structural units, thereby amplifying the birefringence. Detailed theoretical calculations show that the $(PO_3F)^{2-}$ and $(PO_2F_2)^-$ anions contribute to the linear optical properties and ultra-wide bandgap of $KBaSr(PO_2F_2)(PO_3F)_2$.

Data availability

All data supporting this article have been included within the manuscript and ESI.† Crystallographic data for $KBaSr(PO_2F_2)(PO_3F)_2$ have been deposited at the CCDC under number 2428547. The article provides sufficient experimental evidence and data to ensure reproducibility of the work.

Conflicts of interest

The authors declare no competing interests.

Acknowledgements

This work acknowledges the financial support from the National Natural Science Foundation of China (22193042 and 22405273), the Natural Science Foundation of Fujian Province (2022J02012), the Key Research Program of Frontier Sciences of the Chinese Academy of Sciences (ZDBS-LY-SLH024), the Postdoctoral Fellowship Program of CPSF under Grant Number GZB20240747, and the China Postdoctoral Science Foundation (2023M743498).

References

1 C. Jin, X. Shi, H. Zeng, S. Han, Z. Chen, Z. Yang, M. Mutailipu and S. Pan, Hydroxyfluorooxoborate $Na[B_3O_3F_2(OH)_2]\cdot[B(OH)_3]$: Optimizing the Optical Anisotropy with Heteroanionic Units for Deep Ultraviolet Birefringent Crystals, *Angew. Chem., Int. Ed.*, 2021, **60**, 20469–20475.
2 Y. Zhou, X. Zhang, M. Hong, J. Luo and S. Zhao, Achieving effective balance between bandgap and birefringence by confining π-conjugation in an optically anisotropic crystal, *Sci. Bull.*, 2022, **67**, 2276–2279.
3 M. Y. Li, X. Liu, Y. C. Liu, R. X. Wang, J. Guo, L. M. Wu and L. Chen, Unprecedented Deep Ultraviolet (DUV) Birefringence in Fluorides Constructed from Linear π-Group Anisotropic Structure Building Units, *Angew. Chem., Int. Ed.*, 2025, **64**, e202423054.
4 M. J. Dodge, Refractive properties of magnesium fluoride, *Appl. Opt.*, 1984, **23**, 1980–1985.
5 Y. Q. Li, X. Zhang, Y. Zhou, W. Q. Huang, Y. P. Song, H. Wang, M. J. Li, M. C. Hong, J. H. Luo and S. G. Zhao, An Optically Anisotropic Crystal with Large Birefringence Arising from Cooperative π Orbitals, *Angew. Chem., Int. Ed.*, 2022, **61**, e202208811.
6 Y. Q. Li, X. Zhang, J. Y. Zheng, Y. Zhou, W. Q. Huang, Y. P. Song, H. Wang, X. Y. Song, J. H. Luo and S. E. Zhao, A Hydrogen Bonded Supramolecular Framework Birefringent Crystal, *Angew. Chem., Int. Ed.*, 2023, **62**, e202304498.
7 Y. C. Liu, X. M. Liu, S. Liu, Q. R. Ding, Y. Q. Li, L. N. Li, S. G. Zhao, Z. S. Lin, J. H. Luo and M. C. Hong, An Unprecedented Antimony(III) Borate with Strong Linear and Nonlinear Optical Responses, *Angew. Chem., Int. Ed.*, 2020, **59**, 7793–7796.
8 Y. L. Deng, L. Huang, X. H. Dong, L. Wang, K. M. Ok, H. M. Zeng, Z. E. Lin and G. H. Zou, $K_2Sb(P_2O_7)F$: Cairo Pentagonal Layer with Bifunctional Genes Reveal Optical Performance, *Angew. Chem., Int. Ed.*, 2021, **60**, 3856–3857.
9 Z. P. Du, X. Y. Song, W. Liu, Z. Y. Wang, H. Y. Sha, Q. T. Xu, Y. Zhou, Y. Q. Li, J. H. Luo and S. E. Zhao, Combining rigid and deformable groups to construct a robust birefringent crystal for compact polarization components, *Sci. Bull.*, 2024, **69**, 2205–2211.
10 X. Dong, L. Huang, H. Zeng, Z. Lin, K. M. Ok and G. Zou, High-Performance Sulfate Optical Materials Exhibiting Giant Second Harmonic Generation and Large Birefringence, *Angew. Chem., Int. Ed.*, 2022, **61**, e202116790.
11 S. Choi, Y. Li, Y. Kuk and K. M. Ok, $(NH_4)_2Cd_2Cl_3F_3$ and $(NH_4)_2Cd_2Br_3F_3$: The First Fluoride-Containing d^{10} Metal Mixed Halides Exhibiting Superior Ultraviolet Nonlinear Optical Properties, *Adv. Sci.*, 2025, 2414503.

Published on 09 maggio 2025. Downloaded on 06/05/2026 19:58:39.

12 W. Q. Huang, S. G. Zhao and J. H. Luo, Recent Development of Non-π-Conjugated Deep Ultraviolet Nonlinear Optical Materials, *Chem. Mater.*, 2022, **34**, 5–28.
13 X. Chen, Y. Q. Li, J. H. Luo and S. G. Zhao, Recent advances in non-π-conjugated nonlinear optical sulfates with deep-UV absorption edge, *Chin. J. Struct. Chem.*, 2023, **42**, 100044.
14 W. Jungowska and T. Znamierowska, Studies on thermal-stability of mixes metaphosphates $KLa(PO_3)_4$ and $K_2La(PO_3)_5$, *J. Therm. Anal.*, 1990, **36**, 2095–2098.
15 S. E. Zhao, P. F. Gong, S. Y. Luo, L. Bai, Z. S. Lin, C. M. Ji, T. L. Chen, M. C. Hong and J. H. Luo, Deep-Ultraviolet Transparent Phosphates $RbBa_2(PO_3)_5$ and $Rb_2Ba_3(P_2O_7)_2$ Show Nonlinear Optical Activity from Condensation of $[PO_4]^{3-}$ Units, *J. Am. Chem. Soc.*, 2014, **136**, 8560–8563.
16 L. L. Wu, H. T. Tian, C. S. Lin, X. Zhao, H. X. Fan, P. X. Dong, S. D. Yang, N. Ye and M. Luo, Optimized arrangement of non-π-conjugated PO_3NH_3 units leads to enhanced ultraviolet optical nonlinearity in $NaPO_3NH_3$, *Inorg. Chem. Front.*, 2024, **11**, 1145–1152.
17 B. Zhang, E. Tikhonov, C. Xie, Z. Yang and S. Pan, Prediction of Fluorooxoborates with Colossal Second Harmonic Generation (SHG) Coefficients and Extremely Wide Band Gaps: Towards Modulating Properties by Tuning the BO_3/BO_3F Ratio in Layers, *Angew. Chem., Int. Ed.*, 2019, **58**, 11726–11730.
18 J. Lu, J. N. Yue, L. Xiong, W. K. Zhang, L. Chen and L. M. Wu, Uniform Alignment of Non-π-Conjugated Species Enhances Deep Ultraviolet Optical Nonlinearity, *J. Am. Chem. Soc.*, 2019, **141**, 8093–8097.
19 M. Luo, C. Lin, D. Lin and N. Ye, Rational Design of the Metal-Free $KBe_2BO_3F_2$□(KBBF) Family Member $C(NH_2)_3SO_3F$ with Ultraviolet Optical Nonlinearity, *Angew. Chem., Int. Ed.*, 2020, **59**, 15978–15981.
20 W. Y. Zhang, Z. L. Wei, Z. H. Yang and S. L. Pan, Two new ammonium/alkali-rare earth metal difluorophosphates $ALa(PO_2F_2)_4$ (A = NH_4 and K) with moderate birefringence and short cutoff edges, *Dalton Trans.*, 2020, **49**, 11591–11596.
21 W. Q. Jin, C. W. Xie, X. L. Hou, M. Cheng, E. Tikhonov, M. F. Wu, S. L. Pan and Z. H. Yang, From Monofluorophosphates A_2PO_3F to Difluorophosphates APO_2F_2 (A = alkali metal): Design of a Potential Deep-Ultraviolet Nonlinear Optical Materials System with a Shortened Phase-Matching Wavelength, *Chem. Mater.*, 2023, **35**, 5281–5290.
22 W. Y. Zhang, W. Q. Jin, M. Cheng, R. N. Zhang, Z. H. Yang and S. L. Pan, From centrosymmetric to noncentrosymmetric: effect of the cation on the crystal structures and birefringence values of $(NH_4)_{n-2}AE(PO_2F_2)_n$ (AE = Mg, Sr and Ba, n=2, 3 and 4), *Dalton Trans.*, 2021, **50**, 10206–10213.
23 W. M. Dong, Y. J. Sun, H. H. Feng, D. Z. Deng, J. Jiang, J. Yang, W. Guo, L. B. Tang, J. C. Kong and J. Zhao, $K_2Sr_4(PO_3)_{10}$: A Polyphosphate with Deep-UV Cutoff Edge and Enlarged Birefringence, *Inorg. Chem.*, 2023, **62**, 16215–16221.
24 H. Yang, J. Hwang, Y. Tonouchi, K. Matsumoto and R. Hagiwara, Sodium difluorophosphate: facile synthesis, structure, and electrochemical behavior as an additive for sodium-ion batteries, *J. Mater. Chem. A*, 2021, **9**, 3637–3647.
25 Q. R. Ding, X. Y. Zhang, Z. S. Lin, Z. Y. Xiong, Y. S. Wang, X. F. Long, S. G. Zhao, M. C. Hong and J. H. Luo, Designing a deep-UV nonlinear optical monofluorophosphate, *Sci. China Mater.*, 2022, **65**, 1710–1714.
26 S. S. Chen, Z. Y. Bai, X. Y. Song, T. Ouyang, Y. Q. Li, Q. R. Ding, H. Wang, W. T. Chen, J. H. Luo and S. E. Zhao, A HTO-Type Nonlinear Optical Fluorophosphate with Ultrawide Bandgap, *Small*, 2025, **21**, 2408191.
27 R. Ishikawa, R. Kano, T. Bando, Y. Suematsu, S. Ishikawa, M. Kubo, N. Narukage, H. Hara, S. Tsuneta, H. Watanabe, K. Ichimoto, K. Aoki and K. Miyagawa, Birefringence of magnesium fluoride in the vacuum ultraviolet and application to a half-waveplate, *Appl. Opt.*, 2013, **52**, 8205–8211.
28 Y. Y. Yang, Y. Guo, Y. G. Chen, X. W. Hu, X. Zhang and X. M. Zhang, Hexameric poly-fluoroberyllophosphate $Na_4Be_2PO_4F_5$ with moderate birefringence and deep-ultraviolet transmission as a potential zero-order-waveplate crystal, *Inorg. Chem. Front.*, 2022, **9**, 5469–5477.
29 J. Y. Hu, Z. J. Ma, J. Li, C. He, Q. H. Li and K. C. Wu, Strain engineering of nonlinear boron phosphate for phase matching in the ultraviolet region: a first-principles study, *J. Phys. D:Appl. Phys.*, 2016, **49**, 185103.
30 Y. G. Shen, Y. Yang, S. G. Zhao, B. Q. Zhao, Z. S. Lin, C. M. Ji, L. N. Li, P. Fu, M. C. Hong and J. H. Luo, Deep-Ultraviolet Transparent Cs_2LiPO_4 Exhibits an Unprecedented Second Harmonic Generation, *Chem. Mater.*, 2016, **28**, 7110–7116.
31 H. W. Yu, J. Young, H. P. Wu, W. G. Zhang, J. M. Rondinelli and P. S. Halasyamani, $M_4Mg_4(P_2O_7)_3$ (M = K, Rb): Structural Engineering of Pyrophosphates for Nonlinear Optical Applications, *Chem. Mater.*, 2017, **29**, 1845–1855.
32 Y. Zhong, P. Shan, T. Sun, Z. Hu, H. Liu, S. Liu, Y. Kong and J. Xu, Growth and theoretical study on the deep-ultraviolet transparent β-$CsBa_2(PO_3)_5$ nonlinear optical crystal, *CrystEngComm*, 2019, **21**, 4690–4695.
33 Z. Y. Bai, L. H. Liu, L. Z. Zhang, Y. S. Huang, F. F. Yuan and Z. B. Lin, $K_2SrP_4O_{12}$: a deep-UV transparent cyclophosphate as a nonlinear optical crystal, *Chem. Commun.*, 2019, **55**, 8454–8457.
34 J. Chen, L. Xiong, L. Chen and L. M. Wu, $Ba_2NaClP_2O_7$: Unprecedented Phase Matchability Induced by Symmetry Breaking and Its Unique Fresnoite-Type Structure, *J. Am. Chem. Soc.*, 2018, **140**, 14082–14086.
35 J. Durand, W. Granier, L. Cot and J. L. Galigne, Structural studies of oxyfluoride compounds of PV .3. crystal-structure of $NaK_3(PO_3F)_2$, *Acta Cryst. B*, 1975, **31**, 1533–1535.
36 X. R. Yang, X. Liu, Z. J. Wang, X. B. Deng, H. J. Lu, Y. J. Li, X. F. Long, L. Chen and L. M. Wu, $Na_{1.5}Rb_{0.5}PO_3F{\cdot}H_2O$: synthesis, properties, and stepwise reconstruction of the hydrogen bond network, *Inorg. Chem. Front.*, 2021, **8**, 4544–4552.

 This journal is © the Partner Organisations 2025

37 L. Voon, In-plane birefringence of asymmetric (001) quantum wells, *Appl. Phys. Lett.*, 1997, **70**, 2446–2448.
38 Y. R. Chen, X. C. Zhu, S. H. Ma, H. W. Yu, H. P. Wu, Z. G. Hu and Y. C. Wu, Effective third harmonic generation of 355 nm ultraviolet laser based on the borate-phosphate $Ba_3(ZnB_5O_{10})PO_4$ crystal, *Opt. Mater. Express*, 2023, **13**, 3164–3172.
39 L. Xiong, J. Chen, J. Lu, C. Y. Pan and L. M. Wu, Monofluorophosphates: A New Source of Deep-Ultraviolet Nonlinear Optical Materials, *Chem. Mater.*, 2018, **30**, 7823–7830.
40 J. Chen, L. Xiong, L. Chen and L.-M. Wu, $Ba_2NaClP_2O_7$: Unprecedented Phase Matchability Induced by Symmetry Breaking and Its Unique Fresnoite-Type Structure, *J. Am. Chem. Soc.*, 2018, **140**, 14082–14086.
41 C. Y. Pan, X. R. Yang, L. Xiong, Z. W. Lu, B. Y. Zhen, X. Sui, X. B. Deng, L. Chen and L. M. Wu, Solid-State Nonlinear Optical Switch with the Widest Switching Temperature Range Owing to Its Continuously Tunable T_c, *J. Am. Chem. Soc.*, 2020, **142**, 6423–6431.
42 S. J. Clark, M. D. Segall, C. J. Pickard, P. J. Hasnip, M. J. Probert, K. Refson and M. C. Payne, First principles methods using CASTEP, *Z. Kristallogr.*, 2005, **220**, 567–570.
43 W. Kohn, Nobel Lecture: Electronic structure of matter-wave functions and density functionals, *Rev. Mod. Phys.*, 1999, **71**, 1253–1266.
44 J. P. Perdew, K. Burke and M. Ernzerhof, Generalized gradient approximation made simple, *Phys. Rev. Lett.*, 1996, **77**, 3865–3868.
45 H. J. Monkhorst and J. D. Pack, Special Points for Brillouin-Zone Integrations, *Phys. Rev. B*, 1976, **13**, 5188–5192.

Published on 09 maggio 2025. Downloaded on 06/05/2026 19:58:39.